RSC Advances

PAPER

View Article Online
View Journal | View Issue

Cite this: *RSC Adv.*, 2019, **9**, 34642

Mechanical and thermal properties and cytotoxicity of Al_2O_3 nano particle-reinforced poly(ether-ether-ketone) for bone implants

Tianyue Wei,[a] Jin Wang,[a] Xunzhi Yu,[a] Youfa Wang,*[ab] Qingzhi Wu *[ab] and Chang Chen[a]

Weak mechanical properties and mismatching of elastic modulus to human bone restricts the use of PEEK as a bone implant material. By introducing reinforcing particles in polymers, composite material properties could be tailored to meet specific design requirements. In this work, composite materials with PEEK as a matrix and Al_2O_3 as reinforcing fillers were prepared by an injection molding method. Subsequently, the effects of different particle sizes (30 nm, 0.2 μm, 5 μm) and distinct contents (2.5 wt%, 5.0 wt%, 7.5 wt%, 10.0 wt%, 12.5 wt%, 15.0 wt%) of Al_2O_3 powder on the mechanical properties of the composites, such as tensile strength, bending strength, impact strength, Vickers hardness and modulus, were investigated by an electronic universal testing machine. Thermogravimetric analysis (TGA) and differential scanning calorimetry (DSC) were used to compare the thermal properties of composites with different proportions. Besides, the cross-section fractography of the composites after the tensile strength test was characterized by scanning electron microscopy (SEM) to analyze the interface bonding effect. Moreover, mouse fibroblast L929 cells were used for cytotoxicity testing of CCK-8 kit to evaluate cell compatibility of the composite *in vitro* and cell morphology was observed by inverted fluorescence microscopy. Based on the obtained results, Al_2O_3 reinforcement enhanced many properties in some aspects, which makes the Al_2O_3/PEEK composite one of the most promising candidates for human bone implantation, reconstruction, orthopedic and trauma applications.

Received 10th July 2019
Accepted 8th October 2019

DOI: 10.1039/c9ra05258e

rsc.li/rsc-advances

1 Introduction

Poly(oxy-1,4-phenyleneoxy-1,4-phenylenecarbonyl-1,4-phenylene) more commonly known as poly(ether-ether-ketene) (PEEK) is a fully aromatic semi-crystalline thermoplastic engineering plastic. The macromolecular chain contains a rigid benzene ring, flexible ether bonds and carbonyl groups that improve the intermolecular interactions, giving this high-performance polymer high strength, high modulus, high fracture toughness, and other excellent comprehensive performance.[1] Apart from that, it also could retain its mechanical structure in harsh environments since PEEK has high chemical resistance and high thermal stability.[2] In 1962, Bonner first introduced a method of preparation for this high-performance polymer.[3] Since then, it has been widely used in various fields such as automotive parts, semiconductor, aerospace, petrochemical, machinery, medical apparatus and instruments, electrical and electronic equipment. PEEK has good biocompatibility and solvent resistance; even if it undergoes X-ray irradiation and high temperature ethylene oxide sterilization repeatedly, it can maintain its original mechanical properties.[4] By the late 1990s, PEEK became the most promising candidate for replacing metal implant components especially in medical apparatus and instruments since metals and their alloys had serious problems of noxiousness of the released metal ions and stress shielding effects.[5,6] Mechanical properties and biocompatibility of PEEK and its composites have been extensively studied.[7,8] The results show that compared to the stainless steel, metal and their alloys (over 100 GPa), PEEK (3–4 GPa) has elastic modulus closer to that of human cortical bone (6–30 GPa), which could mitigate the stress shielding effect strikingly.[9] However, higher mechanical properties are required under some special medical circumstance. By introducing reinforcing particles as well as fibers in polymers, composite material properties can be tailored to meet specific design requirements. Wen Q *et al.* have early reported that PEEK reinforced by carbon fiber (CF-PEEK) were successfully prepared by injection molding method and the mechanical properties especially elastic modulus had been improved remarkably.[10] Other kinds of carbon derivative reinforced composites have also been studied, such as carbon tube and graphene.[11–16] Moreover, Yi D *et al.* reported that a unique PEEK

[a]*State Key Laboratory of Advanced Technology for Materials Synthesis and Processing, Wuhan University of Technology, Wuhan 430070, China. E-mail: wangyoufa@whut.edu.cn; wuqzh@whut.edu.cn*

[b]*Biomedical Materials and Engineering Research Center of Hubei Province, Wuhan University of Technology, Wuhan 430070, China*

bioactive ternary composite, PEEK/n-HA/CF, was developed through a process of compounding, injection, and molding method.[17] This kind of ternary composite not only displayed similar mechanical properties (Young's modulus and elongation) to human cortical bone but also processed the ability to promote cell attachment and proliferation, osteogenic differentiation due to the existence of HA. Linlin H *et al.* have researched on PEEK/ZnO composites, which pointed out that ZnO reinforced PEEK composite exhibited intensive ultraviolet absorption and significant antibacterial activity at pH values in the range of 7–8 even in the absence of light.[18] Apart from that, high-performance PEEK composites reinforced with ceramic particles such as Al_2O_3, AlN, BN, Si_3N_4, SiC, SiO_2, TiO_2, *etc.* also have been studied in recent years.[19,20] There also have been many studies on PEEK surface treatment.[21–25] All these types of fillers could enhance the performance of PEEK in various aspects and some of them meet the functional requirements for bone implant materials. Al_2O_3 nanoparticle has been applied as filler from aerospace to clinical medicine owing to its good mechanical behavior, nontoxicity and cost-effectiveness. Al_2O_3/PEEK composite is one of the most promising candidates for human bone implantation, reconstruction, orthopedic and trauma applications.[26,27]

Nevertheless, the preparation, characterization, and properties of Al_2O_3 enhanced PEEK composites as human bone replacement material are rarely reported. Practically, particle shape, particle size, particle distribution, particle loading, type of matrix, and interface between particle and matrix, all those factors have a great influence on the properties of particulate composites. Pan *et al.* have done a series of research to explore the optimum diameter size, mass fraction of filled nanometer Al_2O_3 particles as well as the coupling agents and dispersing methods for combination of Al_2O_3 and PEEK.[28] Kuo *et al.* have studied nano-Al_2O_3 and nano-SiO_2 on PEEK's mechanical and thermal properties.[3] The report focused more on the comparison between nano-Al_2O_3 and nano-SiO_2 as filler material. Those researches all emphasized the improvement in mechanical and thermal properties, however, less report emphasized the effect of multiple type and content on the cytotoxicity of Al_2O_3 reinforced PEEK composite. In addition, nano sizes of Al_2O_3 particle fillers are more likely to form agglomerations in polymer composites because the van der Waals forces.[29] Accordingly, to explore the effect of content and type of Al_2O_3 particle on mechanical properties, thermal stability, cytotoxicity of Al_2O_3/PEEK composites, and to investigate a better way for dispersing fillers into matrix, we attempted to prepare a variety of Al_2O_3/PEEK composites with different particle sizes (30 nm, 0.2 μm, 5 μm) and distinct contents (2.5 wt%, 5.0 wt%, 7.5 wt%, 10.0 wt%, 12.5 wt%, 15.0 wt%). Besides, their properties were characterized and compared detailedly. The mechanical properties of the composites, tensile strength, bending strength, impact strength, Vickers hardness as well as modulus, were investigated by electronic universal testing machine. Subsequently, thermogravimetric analysis (TGA) and differential scanning calorimetry (DSC) was used to compare the thermal properties of composites with different proportions. Besides, the cross-section fractography of the composites after the tensile strength test was characterized by scanning electron microscopy (SEM) so as to analyse the interface bonding effect. Meanwhile, mouse fibroblast L929 cells were used for cytotoxicity test of CCK-8 kit to evaluate cell compatibility of the composite *in vitro* and cell morphology was observed by inverted fluorescence microscope.

2 Experimental

2.1. Materials

The commercial PEEK powders purchased from VICTREX PEEK Polymer Ltd, UK was used as polymer matrix with an average particle diameter of 50 μm. The weight-average molecular weight M_w of PEEK is 10 600, and the number-average molecular weight M_n of PEEK is 37 000. The commercial α-Al_2O_3 powders with an average particle diameter of 30 nm, 0.2 μm and 5 μm respectively used as filler materials was purchased from Aladdin Industrial Corporation, China. As received ethanol purchased from Sinopharm Chemical Reagent Co Ltd, China was used for homogenizing filler materials and PEEK matrix.

2.2. Preparation of Al_2O_3/PEEK composites

The sample was prepared according to following various steps: the raw material, PEEK and Al_2O_3 powders were firstly dried in a vacuum oven at 120 °C for 12 h (or at 150 °C for 3 h) to remove the residual moisture completely, and then dried Al_2O_3 powder was well premixed in absolute alcohol medium through magnetic stirring for 1 h, meanwhile PEEK powder was blended slowly into the suspended solution with concurrent stirring.[30,31] The mixed solution was stirred continuously at room temperature for another 1 h, which resulted in PEEK/Al_2O_3 slurry. The slurry was suspended under ultrasonic bath for 2 h in order to break down the agglomerates. The resultant homogenous PEEK/Al_2O_3 slurry was dried in an ordinary oven at 80 °C for 12 h.[31] Finally the dried mixed powder was blended in a ball mill for 2 h.[32] Additionally three different size (3 mm, 8 mm, 15 mm in diameter and the proportion of them is 1 : 3 : 6) of ZrO_2 balls were added into the mill machine to mill mixed powder thoroughly.[28]

A series of PEEK/Al_2O_3 composite samples with different Al_2O_3 particle size (30 nm, 0.2 μm, 5 μm) as well as content (2.5 wt%, 5.0 wt%, 7.5 wt%, 10.0 wt%, 12.5 wt%, 15.0 wt%) were fabricated by injection molding method. Prior to this procedure, processed composite powder was firstly dried at 120 °C for 12 h to remove excess alcohol. During injection molding procedure, nozzle temperature was set at 390 °C higher than the PEEK matrix melting temperature T_m (343 °C), to facilitate composite material flow in the mold, which was maintained at 220 °C.[33] Pure PEEK without Al_2O_3 was also fabricated in the same way as control.

2.3. Thermal properties test

The thermal properties including thermal decomposition temperature and melting temperature was studied by Netzsch STA (simultaneous thermal analysis, STA449F3, NETZSCH Scientific Instruments Trading (Shanghai) Ltd, China), which

combined thermogravimetric analysis (TG) with differential scanning calorimeter (DSC). TG and DSC information could be obtained synchronously by using the same sample in the same measurement. Approximately 4–10 mg sample was placed on the pan and was heated from 40 °C to 800 °C with a heating rate of 10 °C min^{-1} to burn the mixture under a nitrogen atmosphere.

2.4. X-ray diffraction measurements (XRD)

The interaction between fillers and PEEK matrix was examined through X-ray diffraction (XRD). The experimental data was obtained by using Empyrean from Malvern Panalytical, China. CuK_α radiation was applied to qualitatively investigate crystallization degree of both Al_2O_3/PEEK composite materials and pure PEEK. Measurement was carried out with 2θ angle varying from 10° to 80° at room temperature.

2.5. Mechanical properties test

Electronic universal testing machine (Instron 5967, Instron (Shanghai) Test Equipment Trading Co Ltd, China) was used to perform quite a few mechanical property evaluations including tensile strength, bending strength, impact strength, and the Vickers hardness test. To be specific, tensile strength was tested according to ISO 527:2012 and the size of each sample was 70 mm × 9 mm × 2 mm. The bending strength test was carried out based on ISO 178:2010 with a sample size of 80 mm × 9 mm × 4 mm. The sample sizes for impact strength are 80 mm × 9 mm × 4 mm and the test for impact strength was performed according to ISO 179-1:2000. Vickers hardness of the sample was measured with Wilson VH1202 Vickers hardness tester (EZ-mat Ltd, China) based on the standard ISO 6507-1:2018. Besides, the values of elastic modulus were obtained from the stress–strain curve. Five duplicate specimens were carried out for each different test and mean values were obtained to ensure the precise result.

2.6. Scanning electron microscopy analysis (SEM)

For a better understanding of the fracture mechanism between fillers and matrix, a JSM-7500F scanning electron microscope (SEM, JEOL Ltd, Japan) was used to evaluate the fractography of tensile specimens. Before observation, the specimens were coated with a thin evaporated layer of gold twice for 40 s by SBC-12 type ion sputtering apparatus (Shanghai Minyi Electronics Co Ltd, China).

2.7. Cytotoxicity test *in vitro*

Cytotoxicity test was carried out under the standard ISO 10993-12:2005. Murine fibroblast L929 cell line (Beijing BeiNaChuangLian Biotechnology Research Institute, China) was used to test the cytotoxicity of composites and pure PEEK. Concretely, these cells were grown in 96-well polystyrene plates containing RPMI 1640 medium (supplemented with 1% mixture of penicillin and streptomycin as well as 10% fetal calf serum) in a humidified air incubator HF90 (Heal Force Development Ltd, China), 95% air and 5% CO_2 at 37 °C for 24 h. Meanwhile, the extract solution of the composites and pure PEEK were obtained by immersing the materials in RPMI 1640 medium for 24 h (at 37 °C). Single-cell suspension was seeded at 5×10^4 cells per 100 μL in each well and after the cells adhere to the wall sufficiently (after 24 h), the cultivate medium was then replaced with the prepared extract solution and incubated for 1 day, 3 days, 5 days and 7 days. 5 samples were evaluated for each group. Besides, the negative control (medium with cells) and the blank control (medium without cells) was also carried on for each plate.[34]

The viability of the cells was evaluated using cell counting assay kit-8 (CCK-8) and before adding CCK-8 solvent, the morphology of cells was observed by inverted fluorescence microscope IX71 (Olympus Corporation, Japan). In detail, 10 μL of the CCK-8 solution was added into each well of the plate and then the cells were incubated in dark for 4–6 h. Next, the absorbance (OD value) of each well was measured at 450 nm using a spectrophotometer 1510 (Thermo Fisher Scientific Ltd, China). To calculate the viability of cells, the blank equation is used:

$$\mathrm{RGR}\ (\%) = \frac{\mathrm{OD_{sample}} - \mathrm{OD_{blank}}}{\mathrm{OD_{negative}} - \mathrm{OD_{blank}}}$$

where OD_{sample} is the mean value of the measured optical density of the test sample. $OD_{negative}$ is the mean value of the measured optical density of the negative group. OD_{blank} is the mean value of the measured optical density of the blanks.

The relative growth rate (RGR) was used to express the cytotoxicity, Table 1 showed the standard for evaluation.

2.8. Statistical analysis

All the quantitative data presented were expressed as mean ± standard deviation and were analyzed using SPSS 22.0 software. A one-way analysis of variance (ANOVA) was used to determine the significant differences among groups. Differences were considered statistically significant at $p \leq 0.05$.

3 Results and discussion

3.1. Thermal properties

Thermal behaviors of pure PEEK and composites were studied by STA. Fig. 1 and 2 showed the TG curves and DSC curves for 3 different composites reinforced by Al_2O_3 particles. Generally, the higher the temperature corresponding to the decrease of the TG curve, the higher the temperature corresponding to the beginning of decomposition, the more stable the material is. The TG results (Fig. 1) illustrated that the thermal stability had been improved owing to the existence of Al_2O_3 fillers. Concretely, the thermal degradation temperature of pure PEEK was 576.0 °C (T_d), however, that of composites reinforced with fillers of the same size, take 5 μm Al_2O_3 particles for example, were increased with filler content (from 576.0 °C to 586.6 °C).[35,36] Obviously, the other two particles (0.2 μm, 30 nm) reinforced composites showed the same trend (from 576 °C to

Table 1 The standard of cytotoxicity determined from RGR

Cytotoxicity level	0	1	2	3	4	5
RGR (%)	≥100	75–99	50–74	25–49	1–24	0

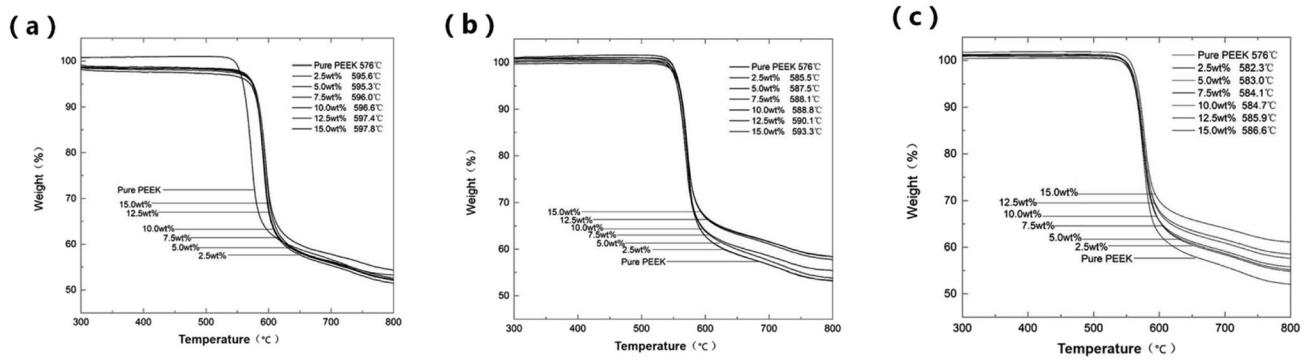

Fig. 1 TGA curves obtained under nitrogen atmosphere of pure PEEK and 3 different types Al_2O_3/PEEK composites: (a) 30 nm Al_2O_3 nanoparticle reinforced, (b) 0.2 μm Al_2O_3 particle reinforced, (c) 5 μm Al_2O_3 particle reinforced.

593.3 °C, from 576 °C to 597.8 °C, respectively). The increase in thermal stability could be due to strong interaction or interfacial bonding between the polymer matrix and the Al_2O_3 particles. Nevertheless, there were differences in degradation temperature between 3 kinds of filler particles reinforced composites of the same mass fraction. In fact, with the same content, the smaller the size of the Al_2O_3 particles, the higher the thermal degradation temperature was. In other words, 30 nm Al_2O_3 particle reinforced composites processed the most excellent thermal stability.

It could be seen from the DSC curves (Fig. 2) obtained from the pure PEEK and Al_2O_3/PEEK composites that all the samples showed a single melting endotherm. The exothermic peak was the melting peak of the samples, and the corresponding temperature of the peak was the melting temperature of the samples (T_m). Moreover, adding Al_2O_3 fillers made the melting peak of composites increased slightly, compared with neat PEEK. The same effect and the probable cause were reported elsewhere.[3]

3.2 XRD analysis

For a better understanding of the interfacial interaction between various contents as well as types of the filler particles and the material matrix, XRD was applied to determine the possible chemical effect. The XRD patterns obtained in Fig. 3 showed that the angular position in the range of $2\theta = 10$–$80°$ of major crystallographic reflection for composite samples conformed to the diffraction pattern of PEEK and Al_2O_3, indicating that there were no extra peaks created or disappeared as compared with raw materials. It seemed that no apparent interaction between fillers and matrix and no appreciable new interfacial phases existed.

In Fig. 3, five sharp diffraction peaks at 18.622°, 20.579°, 22.443°, 25.464° and 28.536° can be attributed to the PEEK and the other several smaller peaks represented the existence of Al_2O_3 particles. The Al_2O_3 diffractions, which represented nano-sized particles, were too low to be resolved in Fig. 3(a). Moreover, the 25.464° diffraction peak for PEEK became extremely weak due to the micro size of Al_2O_3 particle. For the composites with a high fraction of nanoparticles (*e.g.* 15.0 wt%), a lower degree of crystallization might sometimes occur, since the PEEK matrix filled with abundant Al_2O_3 would decrease the mobility of the polymer chain segments during the period of crystallization. Data from Fig. 3(b) showed few changes of diffraction peak shape, which meant the mass fraction of Al_2O_3 content had little effect on the diffraction peak of 0.2 μm Al_2O_3 reinforced composite. As for large grain enhanced PEEK composites (5 μm), the diffraction peak intensity of Al_2O_3 became higher and higher with the addition of Al_2O_3 particles from 2.5 wt% to 15.0 wt% (shown in Fig. 3(c)).

3.3 Mechanical properties

The variations of the average data on the tensile, flexural, impact strength as well as the Young's modulus as a function of particle content were shown in Fig. 4, 5 and Table 2. These

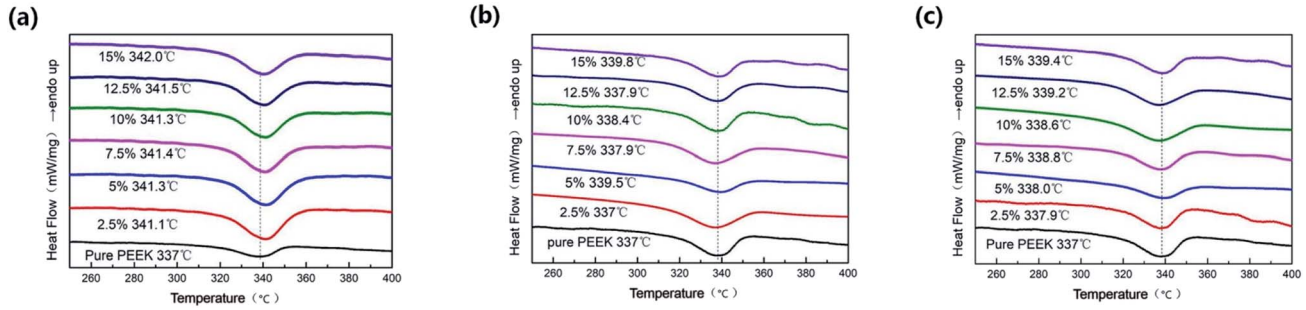

Fig. 2 DSC heating curves of pure PEEK and 3 different types of reinforcement: (a) 30 nm Al_2O_3 nanoparticle reinforced, (b) 0.2 μm Al_2O_3 particle reinforced, (c) 5 μm Al_2O_3 particle reinforced.

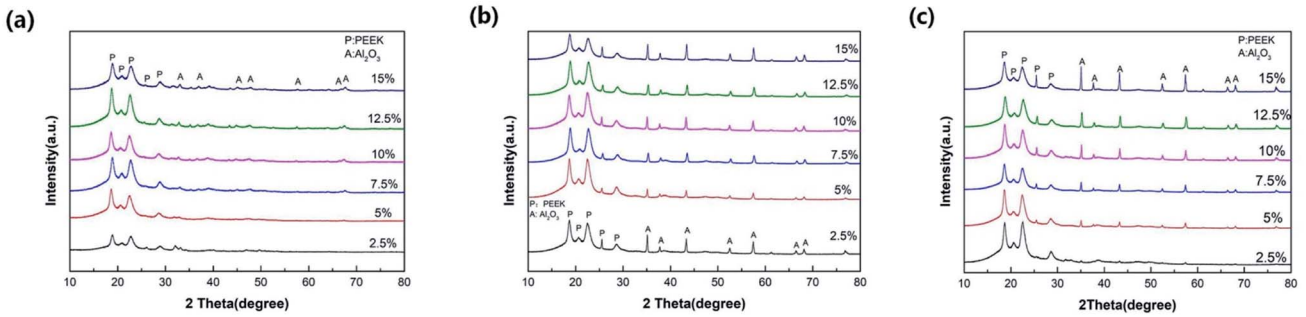

Fig. 3 XRD patterns of the PEEK composites filled with (a) 30 nm Al_2O_3 nanoparticles, (b) 0.2 μm Al_2O_3 particles and (c) 5 μm Al_2O_3 particles.

figures illustrated that mechanical properties of Al_2O_3/PEEK composites had been improved compared with pure PEEK without reinforcement. The tensile strength first increased, and then showed the change trend of decrease. The highest increment occurred in the Al_2O_3 composites with 12.5 wt% 30 nm diameter; raising the PEEK strength from 88.7 up to 99.0 MPa (or an increment percentage of 11.6%, Fig. 4(a)). In comparison, the 0.2 μm and 5 μm Al_2O_3 particles provided a slightly lower improvement in the tensile strength. The trend of Young's modulus was the same as tensile strength, the addition of 30 nm Al_2O_3 particles led to the highest increment from 1782.7 MPa to 1950.2 MPa (Table 2).

It was a remarkable fact that tensile elongations of composites with 5 μm particle reinforcement were relatively lower than the other. The general increasing trend of impact strength was up to 15.0 wt% particles, as depicted in Fig. 4(c). Nevertheless, slight fluctuations could be seen when the content of fillers was 7.5 wt% for 30 nm Al_2O_3 and 5.0 wt% for 5 μm, respectively. Nanometer particles possessed large specific surface area, high surface activity and better interactivity with the polymer chain segment in comparison with normal size particles, so the filling of it could improve the toughness, rigidity and strength of composites. Besides, with the increase of diameter, the specific surface area of inorganic particles would decrease, then lead to the weakening of interaction between inorganic particles and polymer, finally would result in the decrease of tensile and impact strength. Based on that, with the same amount of particles, finer ones especially nano-ones would result in more improvement in tensile and impact properties.

Also, this might be due to the spherical shape of the Al_2O_3 particles, which would usually result in less hindrance when contacting with the polymer segments and more uniform spatial distribution, as well as a lower stress concentration at the particle/matrix interface. All these effects would enable to improve the toughness.

Fig. 4(b) showed the relationships between the bending strength and content of the fillers. The bending strength increased with the weight ratio of Al_2O_3 until it reached the highest peak when Al_2O_3 particles content was 12.5 wt%

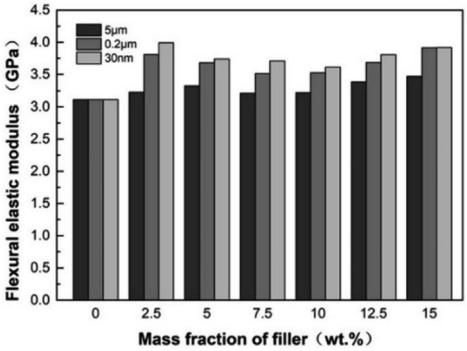

Fig. 5 Comparisons of flexural elastic modulus for 3 types of Al_2O_3 reinforced composites and pure PEEK.

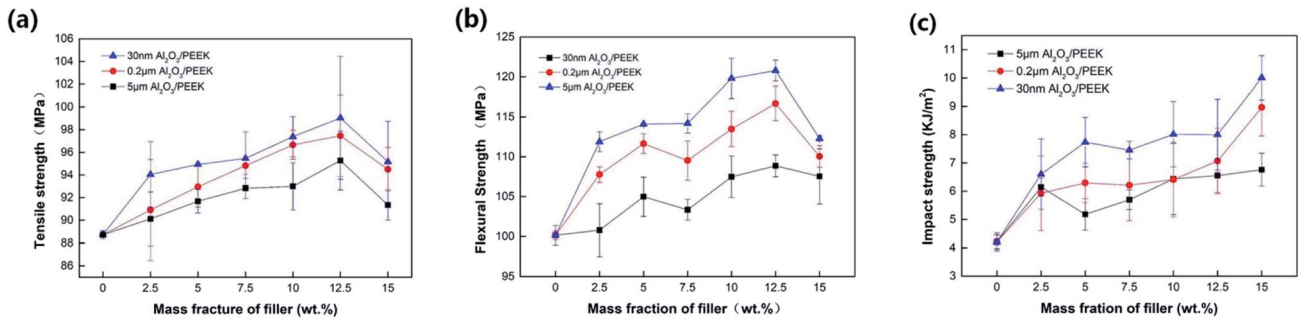

Fig. 4 Tensile strength, flexural strength and impact strength of pure PEEK and Al_2O_3/PEEK composite with different content: (a) tensile strength, (b) flexural strength, (c) impact strength.

Table 2 The mechanical properties of PEEK and Al_2O_3/PEEK composites

Sample type	Mass fraction (%)	Young's modulus (Mpa)	Tensile elongation (%)
Pure PEEK	—	3782.7	51.3
30 nm Al_2O_3/PEEK	2.5	3790.6	48.2
	5.0	3810.3	40.1
	7.5	3878.9	43.8
	10.0	3915.6	45.8
	12.5	3950.2	45.5
	15.0	3853.0	50.1
0.2 μm Al_2O_3/PEEK	2.5	3846.8	21.4
	5.0	3771.1	20.1
	7.5	3850.1	26.2
	10.0	3853.0	25.5
	12.5	3903.1	23.2
	15.0	3912.6	21.1
5 μm Al_2O_3/PEEK	2.5	3842.8	54.1
	5.0	3910.5	19.1
	7.5	3930.6	13.7
	10.0	3884.5	19.8
	12.5	3976.2	10.8
	15.0	3943.1	15.9

although a small reduction occurred at 7.5 wt%. Note that composites with the 5 μm particles consistently exhibited higher flexural strength than that of the 0.2 μm and 30 nm counterparts, suggesting that 5 μm Al_2O_3 fillers supplied with a lower degree of particle clustering and particularly a higher flexibility of PEEK matrix deformation. Specifically, flexural strength of specimen filled with 5 μm Al_2O_3 increased by 20.6% than that of pure PEEK, meanwhile specimen filled with 0.2 μm and 30 nm only increased by 16.5% and 8.6%.

Fig. 5 exhibited the relationships between the flexural elastic modulus and wt% Al_2O_3 of the composites. The flexural elastic modulus of the composites increased to some extent with the addition of Al_2O_3 particles. The flexural modulus of 2.5 wt% for 30 nm reinforced composite were 4 GPa, which represented a increase of 33% compared with the PEEK without reinforcement.

As for the Vickers hardness, Table 3 displayed the hardness value of pure PEEK and composites. The data showed that adding 3 types of Al_2O_3 fillers could improve the Vickers hardness of PEEK matrix by 5–25% and the ability of work. The toughness is a composite index of strength and plasticity. Generally speaking, in combination with the above results, the toughness of the composite strengthened by 30 nm Al_2O_3 particle was the best. The hardness value varied with diameter of Al_2O_3 particles noticeably. To be specific, the 30 nm Al_2O_3 reinforced PEEK composite material had the highest hardness increase. On the contrary, the hardness of 5 μm Al_2O_3 reinforced PEEK composites were not significantly different from that of pure PEEK. On the other hand, for the same kind of particle filler reinforced composites, the different content of filler had little effect on the hardness value. Plasticity was the ability or capacity of a material to undergo irreversible permanent deformation under external forces. Toughness referred to the material before rupture absorbed by plastic deformation work.

3.4 SEM analysis

After the tensile strength test, the cross-section of both composites and pure PEEK was explored by SEM to find the inherent fracture mechanism. Fig. 6 showed a series of representative SEM micrographs of different Al_2O_3 particles with varied content as well as pure PEEK. As Fig. 6(a) and (b)

Table 3 The Vickers hardness value of pure PEEK and composites

Filler diameter	Mass fraction (%)	Hardness value
30 nm	0	21.4 ± 0.9
	2.5	26.0 ± 0.9
	5.0	26.5 ± 0.8
	7.5	26.0 ± 0.3
	10.0	26.1 ± 0.8
	12.5	26.5 ± 0.4
	15.0	26.9 ± 0.7
0.2 μm	0	21.4 ± 0.9
	2.5	25.4 ± 0.1
	5.0	25.3 ± 0.7
	7.5	25.7 ± 0.2
	10.0	25.4 ± 0.9
	12.5	25.7 ± 0.6
	15.0	25.9 ± 0.5
5 μm	0	21.4 ± 0.9
	2.5	21.4 ± 1.6
	5.0	22.2 ± 0.1
	7.5	22.1 ± 1.7
	10.0	22.7 ± 0.4
	12.5	21.6 ± 0.3
	15.0	22.6 ± 0.6

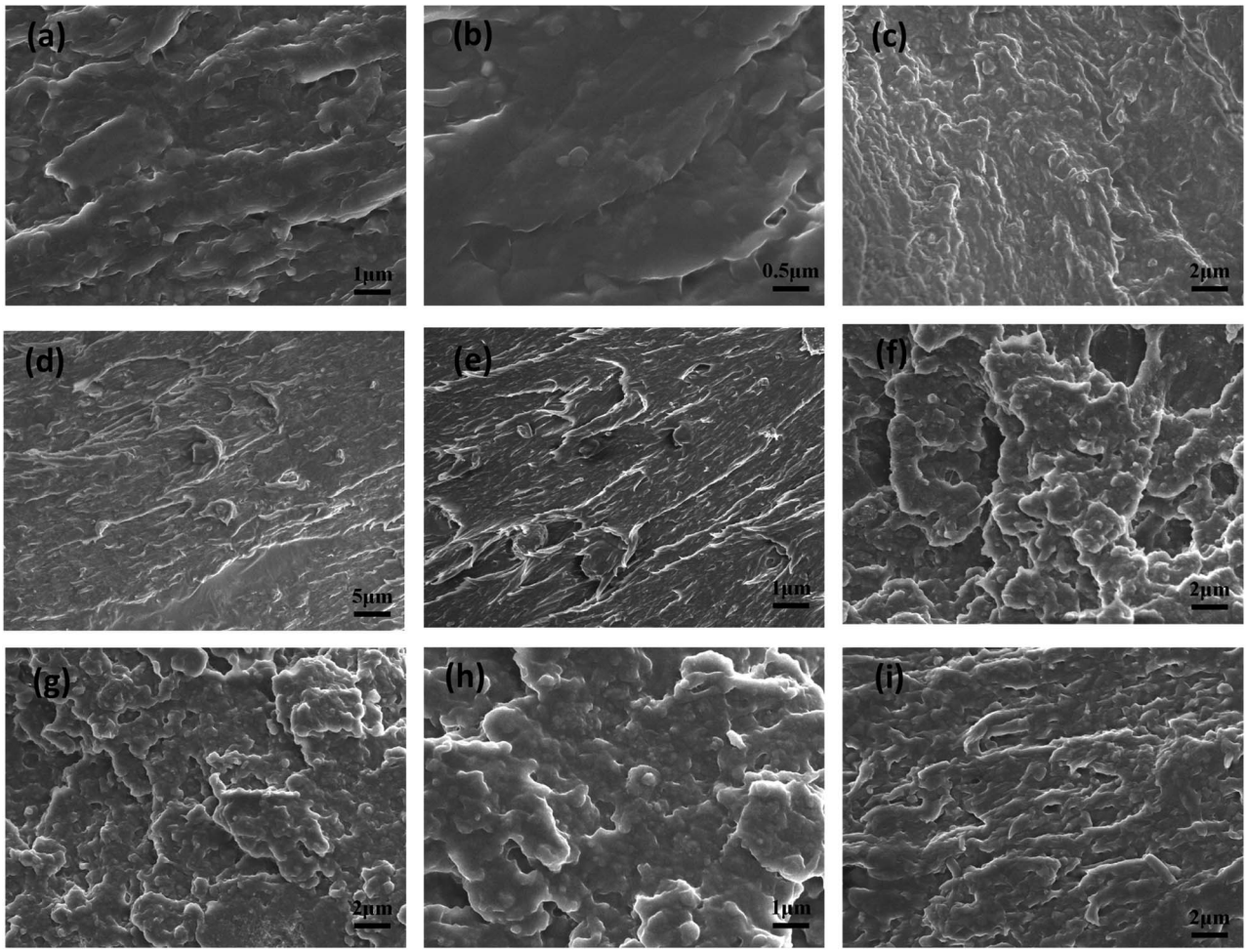

Fig. 6 SEM micrographs with different magnification of tensile fracture surface for PEEK composites filled with 3 different types and various contents Al_2O_3: (a) pure PEEK, (b) pure PEEK, (c) 5% 30 nm Al_2O_3 reinforced, (d) 12.5% 30 nm Al_2O_3 reinforced, (e) 12.5% 30 nm Al_2O_3 reinforced, (f) 12.5% 0.2 μm Al_2O_3 reinforced, (g) 12.5% 0.2 μm Al_2O_3 reinforced, (h) 5% 5 μm Al_2O_3 reinforced, (i) 12.5% 5 μm Al_2O_3 reinforced.

illustrated, the surface of pure PEEK was smooth, and there was almost no visible black hole in the bottom. The random distribution of Al_2O_3 particles at the interface of fracture was observed in Fig. 6(c), (d) and (f)–(h) regardless of diameter of filler particles, which proved that the dispersing method can comminute the conglomeration and disperse it well. Besides, the shapes of Al_2O_3 particles were clearly visible and the black holes were the spaces that the particles were pulled out of, when the composites were broken. As Fig. 6(d) and (e) shown, the rough multilayer structure with distinct edges appeared when composites were reinforced by 30 nm Al_2O_3 particles and the content was up to 12.5 wt%, which could account for the high level of tensile strength since it could increase the area on which the tensile force acts. However, as Fig. 6(c) shown, when the 30 nm Al_2O_3 content was 5 wt%, the fracture showed that the number of layers in the multi-layer structure was significantly reduced, which was also the reason why the tensile strength was not as good as 12.5 wt%. This corresponded to the previous results of tensile strength. The 30 nm particle reinforced composites showed many dimple structures, which represented ductile fracture. Microspores caused by inclusions or coarse sediments were enlarged and the material between them was necked and sheared during further yielding. Further, the depth of these dimples can be considered a measure of the ductility of the material. This fracture had a slow tearing process and consumed energy during the crack propagation, resulting in a series of radioactive cracks. Unfortunately, nanoscale packing agglomeration was serious and common among 30 nm Al_2O_3 particles sample groups, which affected further strengthening of mechanical strength. According to Fig. 6(f) and (g), the fractograph also displayed abundant of layers. Meanwhile, it could be clearly seen that there were remaining PEEK particles in most of the holes which indicated that when the sample was broken, some of the particles were pulled out rather than fracture. On the contrary, according to Fig. 6(h) and (i), there was much less trace of multi-layer structure in fractograph of 0.5 μm Al_2O_3 particles reinforced. Compare 12.5% 5 μm Al_2O_3 reinforced PEEK composite with 5%, it is not difficult to find that multi-layer structures are more obvious. This is also consistent with the results of tensile strength comparison.

3.5 Cytotoxicity test *in vitro*

To explore the cytocompatibility of Al_2O_3/PEEK composites, L929 cells were used and samples were detected with 1, 3, 5 and 7 days cell culture time in the extracts. Fig. 7(a)–(c) showed the cytotoxicity results of CCK-8 assessments. According to the standard 10993-12:2005, the samples were not toxic to cells when the relative growth rate (RGR) value is higher than 75% and when RGR value lays between 50–75%, it represented slight toxicity. It can be seen that the RGR values for 30 nm Al_2O_3/PEEK composites in all period time were higher than 75%, indicating this particle size type reinforced composites had no toxicity to cells. However, 0.2 μm and 5 μm Al_2O_3 reinforced composites both had slight toxic effect on cells based on the fact that RGR value was mostly between 50–75% on the 7 days of experimental period. The reason for the great difference in toxicity between the composites reinforced by different particles may be that the composite with large particle size fillers had poor compatibility at the interface between matrix and fillers, making small amounts of filler molecules precipitate into the extracts. These molecules had bad effects to cells. On the other hand, cell viability was markedly lower than that of pure PEEK after adding all kinds of Al_2O_3 fillers, indicating cell activity decreased due to the existence of Al_2O_3 fillers in a short time. Specifically, Al_2O_3 debris on the surface of the composites is easy to enter the extracts during the preparation of extracts, resulting in the damage to cells. As Fig. 7(a) illustrated, after 7 days' incubation, there was no distinct difference between the viability values of the 30 nm Al_2O_3 reinforced composites and the pure PEEK, proving that the addition of this size of filler did not effect on the cells in the long term. On the contrary, Fig. 7(b) and (c) showed that 0.2 μm and 5 μm Al_2O_3 reinforced composites were slightly cytotoxic to cells, especially 5 μm since the RGR value was almost as low as 58% when the fillers content was 10.0 wt%, 12.5 wt%, 15.0 wt%. Besides, the effect of Al_2O_3 filler contents on cell growth can be neglected regardless of the particle size. The observation of the cell morphology after statistical analysis also showed typical information on cytotoxicity. Fig. 8 presented the morphologies of L929 cells cultured in the extracts after 3 days' incubation with inverted fluorescence microscopy. As Fig. 8 shown, negative control groups exhibited healthy morphologies of cells with spherical and spindle shape,

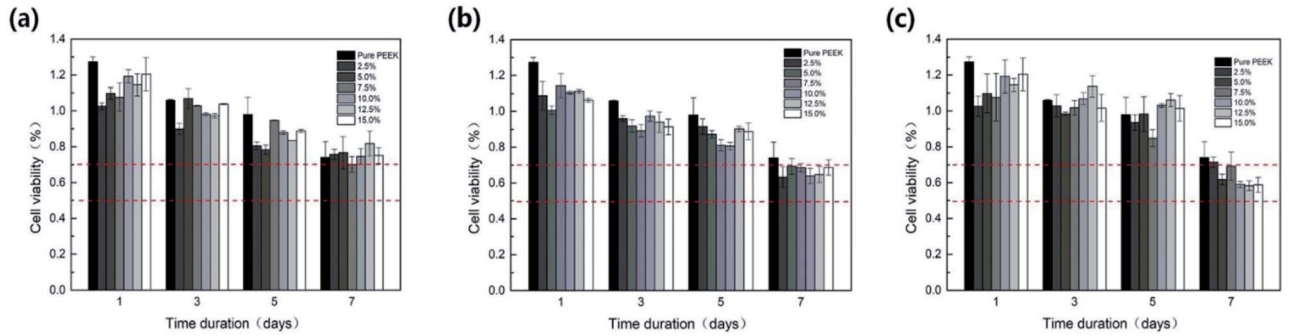

Fig. 7 Cytotoxicity on extracts of the pure PEEK and 3 filler types of Al_2O_3/PEEK composite for 1 day, 3 days, 5 days and 7 days by CCK-8 assay: (a) 30 nm Al_2O_3 reinforcement, (b) 0.2 μm Al_2O_3 reinforcement and (c) 5 μm Al_2O_3 reinforcement.

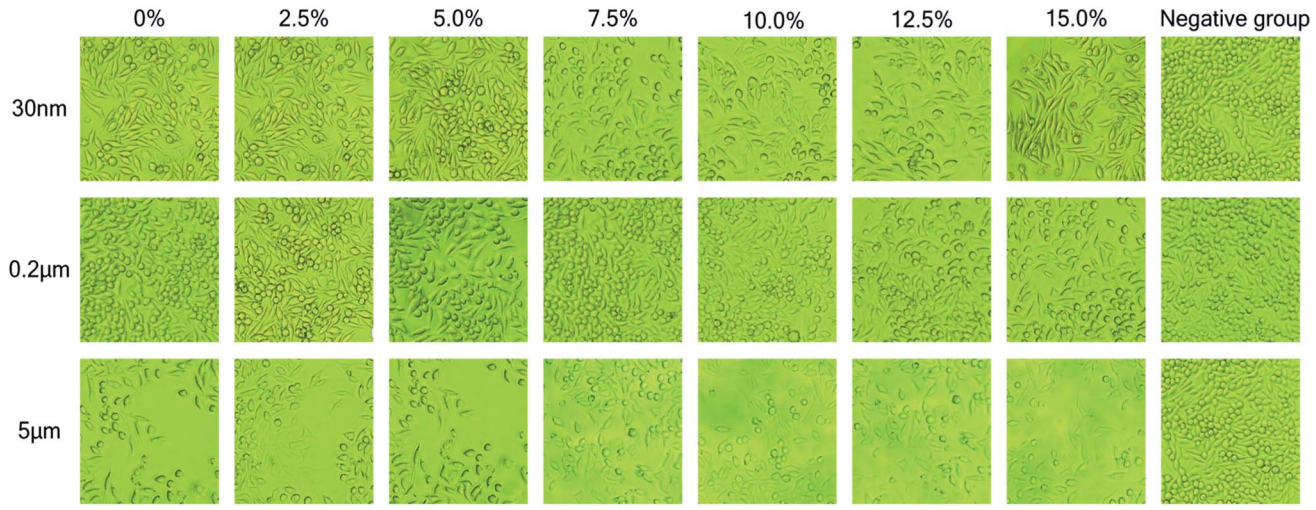

Fig. 8 The morphology of L929 cells incubated in extracts of the pure PEEK and 3 filler types of Al_2O_3/PEEK composite with varied content for 3 days.

which meant good spreading for cells. The cells incubated in pure PEEK and 30 nm Al_2O_3 reinforced composites extracts displayed no difference comparing to negative control groups. Nevertheless, some of the cells incubated in 0.2 μm and 5 μm Al_2O_3 reinforced composites were round, loosely attached or showed changes in morphology; occasional lysed cells were present and slight growth inhibition observable. In general, observation of cell morphology exhibited the same trend as cell cytotoxicity assay.

4 Conclusion

Overall, a variety of Al_2O_3/PEEK composites with different content (2.5 wt%, 5.0 wt%, 7.5 wt%, 10.0 wt%, 12.5 wt%, 15.0 wt%) as well as distinct Al_2O_3 particle diameter size (5 μm, 0.2 μm, 30 nm) were successfully fabricated by injection molding method, which combined various methods of mechanical mixing, ultrasonic dispersing, ball milling dispersing method in order to make the filler evenly dispersed in the matrix. The filling of Al_2O_3 particles resulted in improvement of the thermal decomposition temperature compared with pure PEEK by 10–20 °C. Among them, the addition of 30 nm diameter Al_2O_3 with 15.0 wt% made the most contribution to the thermal stability of the composite. Furthermore, the melting temperature was affected slightly by Al_2O_3 fillers. There is no apparent chemical interaction occurred between the fillers and the PEEK matrix during preparation procedure irrespective of filler types, based on the XRD results. As for mechanical properties, tensile strength, impact strength, flexural strength and Vickers hardness of PEEK reinforced by Al_2O_3 particles were mostly better than those of pure PEEK. The optimum tensile strength improvement occurred in composites filled with 12.5 wt% nanoparticles (30 nm). In addition, 30 nm reinforced composites exhibited better performance in impact strength and Vickers hardness but had lowest flexural strength by comparison. Generally, the variation of modulus was almost in correspondence with that of strength, meanwhile, the tensile elongations of composites with 5 μm particle reinforcement were relatively lower than the other 2 types. Extra particles measuring around 5 μm seemed to elaborate a lower strengthening efficiency in toughness than the 30 nm and 0.2 μm ones, but providing more flexibility and a more uniform spatial distribution. Last but not the least, the addition of Al_2O_3 was proven to deteriorate PEEK marginally in cell viability for the composite based on quantitative measurement of CCK-8 cell cytotoxicity *in vitro* and qualitative comparison of cell morphology image obtained with inverted fluorescence microscopy. Also the result showed 30 nm Al_2O_3 reinforced composites displayed better biocompatibility. Therefore, Al_2O_3/PEEK composites will no doubt expand the applications of PEEK material as bone implantation, reconstruction, orthopedic and trauma field.

Conflicts of interest

The authors declare no conflict of interest.

Acknowledgements

This work was supported by grants from the National Key Research and Development (R&D) Program of China (No. 2018YFB1105700).

References

1 J. M. Toth, M. Wang, B. T. Estes, J. L. Scifert, H. B. Seim 3rd and A. S. Turner, *Biomaterials*, 2006, **27**, 324–334.
2 C. Díaz and G. Fuentes, *Surf. Coat. Technol.*, 2017, **325**, 656–660.
3 M. C. Kuo, C. M. Tsai, J. C. Huang and M. Chen, *Mater. Chem. Phys.*, 2005, **90**, 185–195.
4 L. M. Wenz, K. Memitt, S. A. Brown and A. Moet, *J. Biomed. Mater. Res.*, 1990, **24**, 207–215.
5 K. Abode-Iyamah, S. B. Kim, N. Grosland, R. Kumar, M. Belirgen, T. H. Lim, J. Torner and P. W. Hitchon, *J. Clin. Neurosci.*, 2014, **21**, 651–655.
6 S. Tang, *Int. J. Fatigue*, 2004, **26**, 49–57.
7 Z. Cui, Y. Zhang, Y. Cheng, D. Gong and W. Wang, *Mater. Sci. Eng., C*, 2019, **99**, 1035–1047.
8 K. L. Wong, C. T. Wong, W. C. Liu, H. B. Pan, M. K. Fong, W. M. Lam, W. L. Cheung, W. M. Tang, K. Y. Chiu, K. D. K. Luk and W. W. Lu, *Biomaterials*, 2009, **30**, 3810–3817.
9 L. Wang, S. He, X. Wu, S. Liang, Z. Mu, J. Wei, F. Deng, Y. Deng and S. Wei, *Biomaterials*, 2014, **35**, 6758–6775.
10 W. Qin, Y. Li, J. Ma, Q. Liang and B. Tang, *J. Mech. Behav. Biomed. Mater.*, 2019, **89**, 227–233.
11 C. Lee, X. Wei, J. W. Kysar and J. Hone, *Science*, 2008, **321**, 385–388.
12 C. Rong, G. Ma, S. Zhang, L. Song, Z. Chen, G. Wang and P. M. Ajayan, *Compos. Sci. Technol.*, 2010, **70**, 380–386.
13 E. L. Steinberg, E. Rath, A. Shlaifer, O. Chechik, E. Maman and M. Salai, *J. Mech. Behav. Biomed. Mater.*, 2013, **17**, 221–228.
14 M. Dworak, A. Rudawski, J. Markowski and S. Blazewicz, *Compos. Struct.*, 2017, **161**, 428–434.
15 M. Regis, A. Bellare, T. Pascolini and P. Bracco, *Polym. Degrad. Stab.*, 2017, **136**, 121–130.
16 B. Chen, S. Berretta, K. Evans, K. Smith and O. Ghita, *Appl. Surf. Sci.*, 2018, **428**, 1018–1028.
17 Y. Deng, P. Zhou, X. Liu, L. Wang, X. Xiong, Z. Tang, J. Wei and S. Wei, *Colloids Surf., B*, 2015, **136**, 64–73.
18 L. Hao, Y. Hu, Y. Zhang, W. Wei, X. Hou, Y. Guo, X. Hu and D. Jiang, *RSC Adv.*, 2018, **8**, 27304–27317.
19 A. O. Adebayo, K. K. Alaneme and A. Oyetunji, *J. Taibah Univ. Sci.*, 2018, **13**, 248–257.
20 A. M. Diez-Pascual and A. L. Diez-Vicente, *ACS Appl. Mater. Interfaces*, 2015, **7**, 5561–5573.
21 D. J. Hickey, B. Lorman and I. L. Fedder, *Colloids Surf., B*, 2019, **175**, 509–516.
22 F. B. Torstrick, A. S. P. Lin, D. Potter, D. L. Safranski, T. A. Sulchek, K. Gall and R. E. Guldberg, *Biomaterials*, 2018, **185**, 106–116.
23 T. Miyazaki, C. Matsunami and Y. Shirosaki, *Mater. Sci. Eng., C*, 2017, **70**, 71–75.

24 K. Gan, H. Liu, L. Jiang, X. Liu, X. Song, D. Niu, T. Chen and C. Liu, *Dent. Mater.*, 2016, **32**, e263–e274.
25 T. Ahmadzada, D. R. McKenzie, N. L. James, Y. Yin and Q. Li, *Thin Solid Films*, 2015, **591**, 131–136.
26 A. J. T. Teo, A. Mishra, I. Park, Y.-J. Kim, W.-T. Park and Y.-J. Yoon, *ACS Biomater. Sci. Eng.*, 2016, **2**, 454–472.
27 S. M. Kurtz and J. N. Devine, *Biomaterials*, 2007, **28**, 4845–4869.
28 P. Guoliang, G. Qiang, T. Aiguo and H. Zhiqiang, *Mater. Sci. Eng., A*, 2008, **492**, 383–391.
29 J. Njuguna, K. Pielichowski and S. Desai, *Polym. Adv. Technol.*, 2008, **19**, 947–959.
30 R. K. Goyal, *J. Nanosci. Nanotechnol.*, 2009, **9**, 6902–6909.
31 R. K. Goyal, Y. S. Negi and A. N. Tiwari, *J. Appl. Polym. Sci.*, 2006, **100**, 4623–4631.
32 M. Hedayati, M. Salehi, R. Bagheri, M. Panjepour and A. Maghzian, *Powder Technol.*, 2011, **207**, 296–303.
33 M. Regis, A. Lanzutti, P. Bracco and L. Fedrizzi, *Wear*, 2018, **408–409**, 86–95.
34 A. Hunter, C. W. Archer, P. S. Walker and G. W. Blunn, *Biomaterials*, 1995, **16**, 287–295.
35 L. O. Dandy, G. Oliveux, J. Wood, M. J. Jenkins and G. A. Leeke, *Polym. Degrad. Stab.*, 2015, **112**, 52–62.
36 M. J. Jenkins, J. N. Hay and N. J. Terrill, *Polymer*, 2003, **44**, 6781–6787.